



Research Article

Two-phase flow of dusty fluid with suspended hybrid nanoparticles over a stretching cylinder with modified Fourier heat flux

R. S. Varun Kumar¹ · R. J. Punith Gowda¹ · R. Naveen Kumar¹ · M. Radhika² · B. C. Prasannakumara¹

Received: 12 November 2020 / Accepted: 10 February 2021 / Published online: 27 February 2021
 © The Author(s) 2021 [OPEN](#)

Abstract

The current paper explores the influence of hybrid nanoparticles on the dusty liquid flow through a stretching cylinder by employing the modified Fourier heat flux law. Two phase model is implemented in the present research to characterise the fluid flow. Molybdenum disulphide and silver are used as nanoparticles suspended in base fluid water. The equations which represent the described flow are changed into a set of ordinary differential equations by opting appropriate similarity variables. The reduced dimensionless nonlinear ODEs are numerically solved out by using Runge–Kutta–Fehlberg fourth fifth order inclusive of shooting approach. The impact of several dimensionless parameters over velocity and thermal gradients are deliberated by using graphs. Graphical illustrations for skin friction are also executed. Result outcome reveals that, rise in values of mass concentration of particle declines the velocity and thermal gradient of both dust and fluid phases and cumulative in curvature parameter upsurges the velocity and thermal gradient within the boundary. Further, the heightening of thermal relaxation parameter enhances the thermal profile of both fluid and dust phases.

Keywords Dusty hybrid nanofluid · Stretching cylinder · Mixed convection · Cattaneo-Christov heat flux

List of symbols

(u, v)	Components of velocity	gr	Mixed convection parameter
(x, r)	Directions	a	Stretching rate
$f'(\eta)$	Dimensionless Fluid velocity	β_t and β_v	Interaction parameters of temperature and velocity of the fluid
Θ	Non-dimensional fluid phase temperature	ν	Kinematic viscosity
μ	Dynamic viscosity	m	Mass of the dust particles
$F'(\eta)$	Dimensionless velocity of dust particle	Gr	Greshof number
ρ	Density	$\tau_v = \frac{m}{k}$	Relaxation time of dust particle
k	Thermal conductivity	C	Specific heat
(ρC_p)	Heat capacitance	Re_x	Local Reynolds number
l	Mass concentration of particles	Γ	Thermal relaxation parameter
K	Stokes drag constant	Ec	Eckert number
T	Temperature	ϕ_1, ϕ_2	Volume fractions
C_f	Skin friction coefficient	δ	Curvature parameter
τ_t	Thermal equilibrium time	Pr	Prandtl number
N	Dust particle density number	γ^*	Relaxation time
f	Fluid	$U_w(x)$	Stretching velocity
L	Reference length	Bi	Biot number

✉ B. C. Prasannakumara, dr.bcprasanna@gmail.com | ¹Department of Studies and Research in Mathematics, Davangere University, Davangere, Karnataka, India. ²Government First Grade College, Kolar Gold Field, Karnataka 563122, India.



R	Radius of the cylinder
bf	Base fluid
p	Dust particles
hnf	Hybrid nanofluid
∞	Ambient
w	Surface
s_1, s_2	Solid particles

1 Introduction

From the past decades, scientists were involved in performing a noteworthy investigation in the fluid flow area with respect to heat transfer process. Invention of special fluids paved a way for obtaining higher efficient energy during heat transfer. Researchers used several techniques and methods to improve efficiency of fluids. These fluids are termed as “nanofluids”, which are prepared by dispersing minute particles of size less than 100 nm in the conventional fluids. In modern science and nanotechnology, the rheological performance of a nanofluid is an essential feature for many applications such as cooling process, Geothermal power extraction, Coolant, Lubrication in automobiles and Microchips cooling. Therefore, significant studies have been performing on these nanofluids. Hayat et al. [1] deliberated the nano liquid flow at stagnation point with Brownian motion. They discussed the demeanour of physical parameters versus different profiles via graphical representation. Flow of a fluid consisting of nanoparticles through a revolving disk was explained by Khan et al. [2]. Kuttan et al. [3] deliberated the performance of four diverse nanoparticles on boundary layer stream through a stretching surface. Vinita and Poply [4] examined the impact of heat generation on nanofluid flow past a stretching cylinder. Mondal et al. [5] examined the impact of viscous dissipation and mixed convection on nanofluid stream past a stretching cylinder. The combination of dual or more nanoparticles which are suspended in a convective liquid yield’s hybrid nanofluid. Enrichment of heat transfer in hybrid nanofluid is mainly caused by fusion of two or more nanoparticles. It is experimentally verified that, hybrid nanofluids offer better thermal behaviour than that of base fluids and single nanoparticle fluids. Recently, Khan et al. [6] considered a fluid flow of consisting two nanometallic substances namely, silicon dioxide and molybdenum disulphide for determining the impact of heat source or sink. Farooq et al. [7] explored optimization of entropy on the flow of nanohybrid fluid through a revolving channel. Manjunatha et al. [8] examined the impact of convective boundary constraints on micropolar hybrid nanofluid stream past a stretching surface. Abbas et al. [9] deliberated the stagnation point stream of a hybrid nanofluid past a stretching cylinder.

The fluid flows along with dust particles have extensive range of mechanical applications like transport processes, cement and steel manufacturing industries, flying ash from thermal plants and chilling consequence of AC’s. The two-phase flows involving solid particles scattered in a nanofluid and hybrid nanofluid are of significant applications in industries. Recently, several researchers scrutinised the fluid flow with dust particles suspension. Turkyilmazoglu [10] provided a mathematical explanation for dusty fluid flow along with the boundary conditions. Manjunatha et al. [11] illustrated the dusty fluid flow through a stretchy cylinder on taking account of heat source. Reddy et al. [12] imposed modified Fourier law to investigate dusty hybrid nanofluid flow over a stretching surface with porous medium. Radhika et al. [13] constructed two-way flow approaching model to investigate energy transport in hybrid dusty nanofluid. Mallikarjuna et al. [14] examined effect of viscous dissipation on dusty hybrid nanofluid stream past a stretching surface. Abdelmalek et al. [15] discussed the heat transference in dusty hybrid nano liquid stream.

The flow of different fluids over a cylinder has gained special interest in research area with many significant uses such as revolving-tube heat exchangers, cooling of electronic apparatus, and drilling of oil wells. Hayat et al. [16] used a stretched cylinder to evaluate mixed convective stream of liquid with appropriate boundary conditions. Khan et al. [17] deliberated the hydromagnetic viscous liquid flow through a cylinder. Waqas et al. [18] inspected the influence of activation energy on the nanoparticle fluid flow generated by a cylinder. The heat transfer in MHD nanofluid stream on taking account of ohmic heating over a stretching cylinder was deliberated by Mishra and Kumar [19]. Mixed convective flow and heat transfer process has enormous engineering applications like, solar cells, drying, electronic cooling devices and many others. The scrutiny of mixed convection is complex due to the convoluted interaction between the free convection with the shear motivated flow. Qayyum et al. [20] studied mixed convective two-dimensional nanofluid flow at a stagnation point over a sheet. The entropy optimization of Eyring Powell liquid flow with nanoparticles was analysed by Alsaedi et al. [21]. Further mixed convective heat transfer is scrutinized here. Akbar et al. [22] schematically illustrated mixed convective stream of nanofluid with various slip conditions. Ramesh et al. [23] deliberated the mixed convective stream of hybrid nanofluid past an upright permeable cylinder.

Fourier’s law has been practically applied for studying heat transfer problems. But the most important complexity of this law is that it yields a parabolic equation of energy, which specifies that primary disturbance has established all over the entire system. To beat this difficulty, Cattaneo modified this law with the help of heat flux relaxation

time. Later on, Christov improved Cattaneo’s proposition with suitable explanation. Further, many authors used the modified Fourier model in their studies. Salahuddin et al. [24] examined the impact of modified Fourier heat flux on Williamson liquid past a stretching sheet. Modified Fourier model was implemented by Khan et al. [25] to estimate the hydromagnetic flow of Carreau liquid through a cylinder. Hussain et al. [26] examined the heat transfer features in viscoelastic liquid past a stretching surface by means of modified Fourier heat flux. Ahmed et al. [27] scrutinised the mixed convective stream of maxwell liquid on taking account of Cattaneo-Christov heat flux. Khan et al. [28] deliberated the impact of modified Fourier heat flux on non-Newtonian liquid stream past a stretching cylinder.

In view of the above literature survey, it is obvious to the best of writer’s knowledge, that no efforts have far been initiated with respect to modified Fourier heat flux effect on 2D-stream of a dusty hybrid nanoliquid over a stretching cylinder with mixed convection which constitutes the novelty of the present work. In this study, we discuss the consequence of hybrid nanoparticles on the dusty fluid flow through a stretching cylinder by utilising the modified Fourier heat flux law. The dusty-fluid expressions for dust and nanoparticles are discussed by using equations [1–6], and are employed with corresponding boundary conditions [7], both the dust and fluid particles are governed by the coupled set of the energy and momentum expressions. Further, we chose Molybdenum disulphide and silver as nanoparticles suspended in carrier liquid water. The governing coupled non-linear PDEs are numerically solved and the outcomes attained are presented graphically and discussed briefly. The solutions presented are not only important for practical applications but also work for further research on an ongoing topic that incorporates more complex physical factors, as quoted in the aforementioned articles in this field.

The structure of the paper consists of five parts: Sect. 1 summarizes a few published investigations and the motives for this investigation; Sect. 2 reviews the methodology used; Sect. 3 describes the Numerical method opted; the outcomes of this study and discussion are presented in Sect. 4; the conclusions and recommendations are given in the last section.

2 Mathematical formulation

Consider a two-dimensional incompressible dusty hybrid nanofluid flow through a stretching cylinder with reference length L and stretching rate a . The stretching velocity is denoted by $U_w(x)$ which is given by $U_w(x) = \frac{ax}{L}$. The axis of the cylinder is treated along the x -axis and radial direction along the r axis. The analysis of heat transfer is done by

considering modified Fourier heat flux and mixed convection. The equations which represent the hybrid nanofluid flow with dust particle suspension on taking account of mixed convection through a stretching cylinder is given by (refer Manjunatha et al. [11]):

2.1 Fluid phase

$$\frac{\partial(ru)}{\partial x} + \frac{\partial(rv)}{\partial r} = 0 \tag{1}$$

$$\left(u \frac{\partial u}{\partial x} + v \frac{\partial u}{\partial r}\right) = \frac{\mu_{hnf}}{\rho_{hnf}} \left(\frac{\partial^2 u}{\partial r^2} + \frac{1}{r} \frac{\partial u}{\partial r}\right) + \frac{KN}{\rho_{hnf}} (u_p - u) + \frac{g(\rho\beta)_{hnf}(T - T_\infty)}{\rho_{hnf}} \tag{2}$$

$$\begin{aligned} \left(u \frac{\partial T}{\partial x} + v \frac{\partial T}{\partial r}\right) + \gamma^* \left(u^2 \frac{\partial^2 T}{\partial x^2} + v^2 \frac{\partial^2 T}{\partial r^2} + 2uv \frac{\partial^2 T}{\partial r \partial x} + u \frac{\partial u}{\partial r} \frac{\partial T}{\partial x} + u \frac{\partial v}{\partial x} \frac{\partial T}{\partial r} + v \frac{\partial u}{\partial x} \frac{\partial T}{\partial x} + v \frac{\partial v}{\partial r} \frac{\partial T}{\partial r}\right) \\ = \frac{k_{hnf}}{(\rho C_p)_{hnf}} \left(\frac{\partial^2 T}{\partial r^2} + \frac{1}{r} \frac{\partial T}{\partial r}\right) + \frac{\rho_p}{(\rho C_p)_{hnf} \tau_v} (u_p - u)^2 + \frac{\rho_p (C_p)_f}{(\rho C_p)_{hnf} \tau_t} (T_p - T) \end{aligned} \tag{3}$$

2.2 Dust phase

$$\frac{\partial(ru_p)}{\partial x} + \frac{\partial(rv_p)}{\partial r} = 0 \tag{4}$$

$$\left(u_p \frac{\partial u_p}{\partial x} + v_p \frac{\partial u_p}{\partial r}\right) = \frac{K}{m} (u - u_p) \tag{5}$$

$$\left(u_p \frac{\partial T_p}{\partial x} + v_p \frac{\partial T_p}{\partial r}\right) = -\frac{C_{pf}}{C_m \tau_T} (T_p - T) \tag{6}$$

Boundary constraints for the proposed problem are:

$$u = U_w, v = 0, -k_{hnf} \frac{\partial T}{\partial x} = \Omega_1 (T_w - T) \text{ at } r = R \\ u \rightarrow 0, u_p \rightarrow 0, v_p \rightarrow v, T \rightarrow T_\infty, T_p \rightarrow T_\infty \text{ as } r \rightarrow \infty \tag{7}$$

The suitable similarity variables are:

$$u = \frac{ax}{L} f'(\eta), v = -\frac{1}{r} \sqrt{\frac{v_f a}{L}} Rf(\eta), \eta = \frac{r^2 - R^2}{2R} \sqrt{\frac{a}{v_f L}}, u_p = \frac{ax}{L} F'(\eta), \\ v_p = -\frac{1}{r} \sqrt{\frac{v_f a}{L}} RF(\eta)\theta(\eta) = \frac{T - T_\infty}{T_w - T_\infty}, \theta_p(\eta) = \frac{T_p - T_\infty}{T_w - T_\infty}$$

where $\rho_{hnf}, \mu_{hnf}, (\rho C_p)_{hnf}, (\rho\beta)_{hnf}$ and k_{hnf} is defined by:

$$\begin{aligned} \frac{\rho_{hnf}}{\rho_f} &= (1 - \phi_2) \left[(1 - \phi_1) + \phi_1 \frac{\rho_{s1}}{\rho_f} \right] + \phi_2 \frac{\rho_{s2}}{\rho_f} \\ \frac{(\rho\beta)_{hnf}}{(\rho\beta)_f} &= (1 - \phi_2) \left[(1 - \phi_1) + \phi_1 \frac{(\rho\beta)_{s1}}{(\rho\beta)_f} \right] + \phi_2 \frac{(\rho\beta)_{s2}}{(\rho\beta)_f} \\ \frac{(\rho C_p)_{hnf}}{(C_p\rho)_f} &= (1 - \phi_2) \left[(1 - \phi_1) + \phi_1 \frac{(\rho C_p)_{s1}}{(\rho C_p)_f} \right] + \phi_2 \frac{(\rho C_p)_{s2}}{(\rho C_p)_f} \\ \mu_{hnf} &= \frac{\mu_f}{(1-\phi_1)^{2.5}(1-\phi_2)^{2.5}} \\ \frac{k_{hnf}}{k_f} &= \frac{k_{s2} + 2k_{bf} - 2\phi_2(k_{bf} - k_{s2})}{k_{s2} + 2k_{bf} + \phi_2(k_{bf} - k_{s2})}, \quad \frac{k_{bf}}{k_f} = \frac{k_{s1} + 2k_f - 2\phi_1(k_f - k_{s1})}{k_{s1} + 2k_f + \phi_1(k_f - k_{s1})} \end{aligned}$$

By using above similarity transformation, the obtained reduced equations are as follow:

$$\varepsilon_1 \left[(2\eta\delta + 1)f'' + 2\delta f' \right] - \left[f'^2 - ff'' \right] + \varepsilon_2 \beta_v (F' - f) + \frac{\varepsilon_2}{\varepsilon_3} gr\theta = 0 \tag{8}$$

$$\varepsilon_4 \left(\frac{k_{hnf}}{k_f} \right) \left[\frac{1}{Pr} \right] \left[(2\delta\eta + 1)\theta'' + 2\delta\theta' \right] + f\theta' + \varepsilon_4 \beta_v Ec (F' - f)^2 + \varepsilon_4 \beta_t (\theta_p + \theta') - \Gamma (f^2\theta'' + ff'\theta') = 0 \tag{9}$$

$$FF'' - F'^2 + \beta_v (F' - F) = 0 \tag{10}$$

$$F\theta'_p - \beta_t \gamma (\theta_p - \theta) = 0 \tag{11}$$

where

$$\begin{aligned} \varepsilon_1 &= \frac{1}{(1-\phi_1)^{2.5}(1-\phi_2)^{2.5} \left[(1-\phi_2) \left[(1-\phi_1) + \phi_1 \frac{\rho_{s1}}{\rho_f} \right] + \phi_2 \frac{\rho_{s2}}{\rho_f} \right]} \\ \varepsilon_2 &= \frac{1}{(1-\phi_2) \left[(1-\phi_1) + \phi_1 \frac{\rho_{s1}}{\rho_f} \right] + \phi_2 \frac{\rho_{s2}}{\rho_f}} \\ \varepsilon_3 &= \frac{1}{(1-\phi_2) \left[(1-\phi_1) + \phi_1 \frac{\rho_{s1}}{(\rho\beta)_f} \right] + \phi_2 \frac{\rho_{s2}}{(\rho\beta)_f}} \\ \varepsilon_4 &= \frac{1}{(1-\phi_2) \left[(1-\phi_1) + \phi_1 \frac{(\rho C_p)_{s1}}{(\rho C_p)_f} \right] + \phi_2 \frac{(\rho C_p)_{s2}}{(\rho C_p)_f}} \end{aligned}$$

The corresponding reduced boundary constraints are:

$$f(0) = 0, f'(0) = 1, \frac{k_{hnf}}{k_f} \theta'(0) = -Bi(1 - \theta(0)) \tag{12}$$

$$f(\infty) = 0, F'(\infty) = 0, F(\infty) - f(\infty) = 0, \theta(\infty) = 0, \theta_p(\infty) = 0 \tag{13}$$

where,

$$\begin{aligned} \beta_t &= \frac{L}{\tau_t a}, \quad \beta_v = \frac{L}{\tau_v a}, \quad \delta = \sqrt{\frac{\nu_f L}{a R^2}}, \quad \gamma = \frac{C_{pf}}{C_m}, \quad Pr = \frac{(\rho C_p)_f \nu_f}{k_f}, \\ Re_x &= \frac{U_w x}{\nu_f}, \quad Gr = \frac{g(\beta)_f (T_w - T_\infty) x^3}{\nu_f^2}, \quad I = \frac{mN}{\rho_f}, \\ gr &= \frac{Gr}{Re_x^2}, \quad \Gamma = \frac{\gamma^* a}{L}, \quad Bi = \frac{\Omega_1}{k_f} \sqrt{\frac{\nu_f L}{a}} \end{aligned}$$

The skin friction coefficient is given by

$$C_f = \frac{\mu_{hnf}}{\rho_f u_w^2} \left(\frac{\partial u}{\partial r} \right)_{r=R} \tag{14}$$

By using non-dimensional variables, we have

$$C_f Re_x^{\frac{1}{2}} = \frac{f''(0)}{(1 - \phi_1)^{2.5} (1 - \phi_2)^{2.5}}, \quad \text{Where } Re_x = \frac{U_w x}{\nu_f} \tag{15}$$

3 Numerical solution

To understand the phenomena of the model, the non-linear differential Eqs. (8–11) with corresponding boundary constraints (12–13) are cracked by applying Runge–Kutta–Fehlberg–45 (RKF-45) technique along with the shooting method. The ordinary differential equations which are coupled, nonlinear with boundary constraints are numerically solved and scrutinized with the help of graphs. To solve these reduced equations, corresponding equations along with boundary conditions are transformed into accompanying arrangement of differential equations in first-order using the replacements $f = y(1), f' = y(2), f'' = y(3), \theta = y(4), \theta' = y(5), F = y(6), F' = y(7),$ and $\theta_p = y(8)$.

$$\begin{aligned} y'(1) &= y(2) \\ y'(2) &= y(3) \\ y'(3) &= \frac{-\varepsilon_1 [2\delta y(3)] + [y(2)^2 - y(1)y(3)] - \varepsilon_2 / \beta_v (y(7) - y(2)) - \frac{\varepsilon_2}{\varepsilon_3} gr y(4)}{\varepsilon_1 (2\eta\delta + 1)} \\ y'(4) &= y(5) \\ y'(5) &= y(6) \\ y'(6) &= y(7) \\ y'(7) &= \frac{y(7)^2 - \beta_v (y(2) - y(7))}{y(6)} \\ y'(8) &= \frac{\beta_t \gamma (y(8) - y(4))}{y(6)} \end{aligned}$$

The Runge Kutta Fehlberg-45 order algorithm is given by:

$$\begin{aligned} k_1 &= hf(t_k, y_k) \\ k_2 &= hf\left(t_k + \frac{1}{4}h, y_k + \frac{1}{4}k_1\right) \\ k_3 &= hf\left(t_k + \frac{3}{8}h, y_k + \frac{3}{32}k_1 + \frac{9}{32}k_2\right) \\ k_4 &= hf\left(t_k + \frac{12}{13}h, y_k + \frac{1932}{2197}k_1 - \frac{7200}{2197}k_2 + \frac{7296}{2197}k_3\right) \\ k_5 &= hf\left(t_k + h, y_k + \frac{439}{216}k_1 - 8k_2 + \frac{3680}{513}k_3 - \frac{845}{4104}k_4\right) \\ k_6 &= hf\left(t_k + \frac{1}{2}h, y_k - \frac{8}{27}k_1 + 2k_2 - \frac{3544}{2565}k_3 + \frac{1859}{4104}k_4 - \frac{11}{40}k_5\right) \\ z_{k+1} &= y_k + \frac{16}{135}k_1 + \frac{6656}{12825}k_3 + \frac{28561}{56430}k_4 - \frac{9}{50}k_5 + \frac{2}{55}k_6 \end{aligned}$$

We have selected a distinct value of η_∞ so that far field boundary constraints are satisfied asymptotically. In this present study, an apt finite value of η_∞ is considered as $\eta_\infty < 7$ in such a way that not only numerical solutions converge but also boundary conditions defined at infinity

Table 1 Comparison of the results for the dimensionless temperature gradient when $\epsilon_1 = \frac{k_{hnt}}{k_f} = 1$, $\delta = \Gamma = \epsilon_2 = \epsilon_4 = 0$

Pr	Grubka and Bobba [29]	Abel and Mahesha [30]	Ali [31]	Ishak et al. [32]	Manjunatha et al. [11]	Present work
1.0	1.3333	1.3333	1.3269	1.3333	1.3333	1.3333
10	4.7969	4.7968	4.7969	4.7969	4.7968	4.7969

Table 2 Thermo physical properties of MoS_2 , Ag and water (Refer Shafie et al. [33])

Physical properties	MoS_2	Ag	H_2O
ρ (kg/m ³)	5.06×10^3	10500	997.1
C_p (J/kg.K)	397.21	235	4179
k (W/m.K)	904.4	429	0.613
$\beta \times 10^{-5}$ (K ⁻¹)	2.8424	1.89	21

satisfy asymptotically. The tolerance for related errors up to 10^{-8} is considered for convergence and the step size is chosen as $\Delta\eta = 0.001$. In addition, the CPU time to measure velocity values (1.34 s) is much shorter than the CPU time to measure temperature values (1.74 s) and the CPU concentration time is 2.01 s. We also compared the numerical results obtained in the present study with corresponding results of the published work. Table 1 is constructed for comparative table of present results with existing work and obtained a good agreement with each other.

4 Results and discussions

This segment treats the outcomes of the mixed convective flow of dusty hybrid Nano liquid over a cylinder on taking account of Cattaneo–Christov heat flux. Two phase model is implemented in the present research to characterise the fluid flow. Here, we chosen Molybdenum disulphide and silver as nanoparticles suspended in water as carrier liquid. A numerical scheme is applied to provide a clear understanding and are sufficient to depict the behaviour of flow profiles, which are strategized and deliberated with the assistance of graphs. The thermo-physical characteristics of nanoparticles and base liquid are introduced in Table 2. In this segment, we emphasis on the reliability of non-dimensional parameters that can contribute to velocity and temperature profiles containing dust and hybrid nanoparticles. The choice of the first guess and the extent of the boundary layer η_∞ depends on the parameters values which are used to find the essential solutions. The values selected in computations are based on associated earlier investigation. The physical parameter values are set and for various values of mass concentration of particles, mixed convection parameter, fluid particles interaction parameter over velocity and thermal gradients of fluid

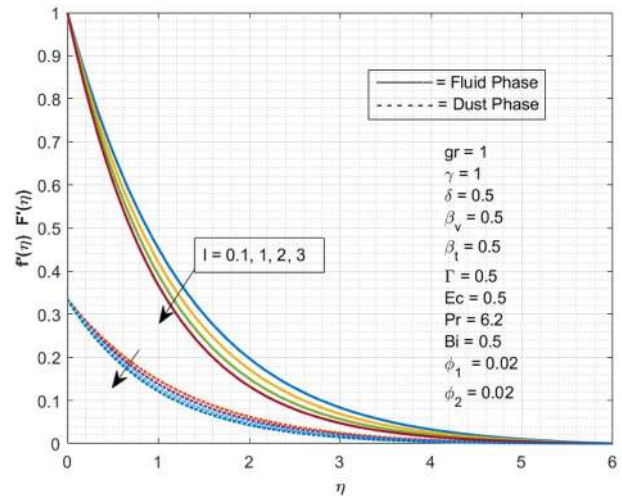


Fig. 1 Power of l over $f'(\eta), F'(\eta)$

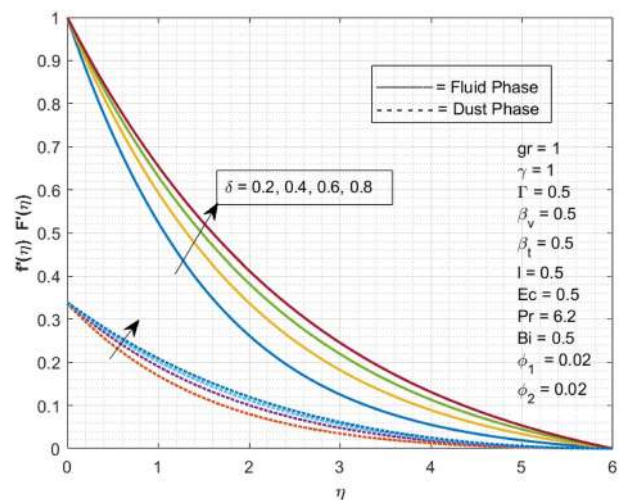


Fig. 2 Power of δ over $f'(\eta), F'(\eta)$

containing dust particles and hybrid nanoparticles. Further, they are exemplified with the help of graphs.

Figure 1 is plotted to see the domination of l over velocity gradient of both fluid and dust phases. The upshot in values of l deteriorates the velocity of both phases as depicted in Fig. 1. It is perceptible that the upsurge in dust particles mass concentration diminishes fluid velocity and related boundary layer thickness. The sway of curvature parameter on velocity gradient of both phases is put on

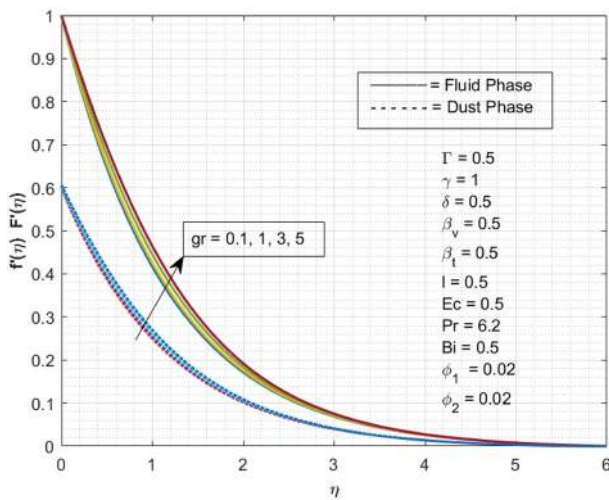


Fig. 3 Power of gr over $f'(\eta), F'(\eta)$

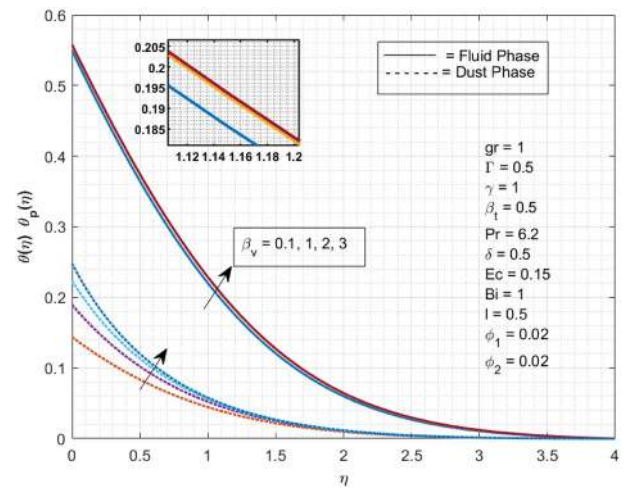


Fig. 5 Power of β_v over $\theta(\eta), \theta_p(\eta)$

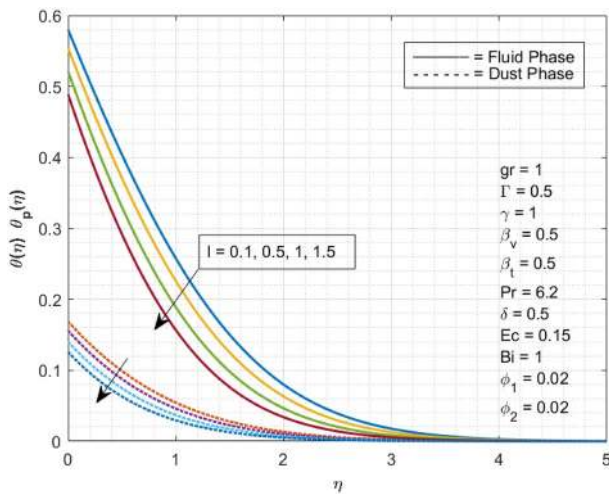


Fig. 4 Power of l over $\theta(\eta), \theta_p(\eta)$

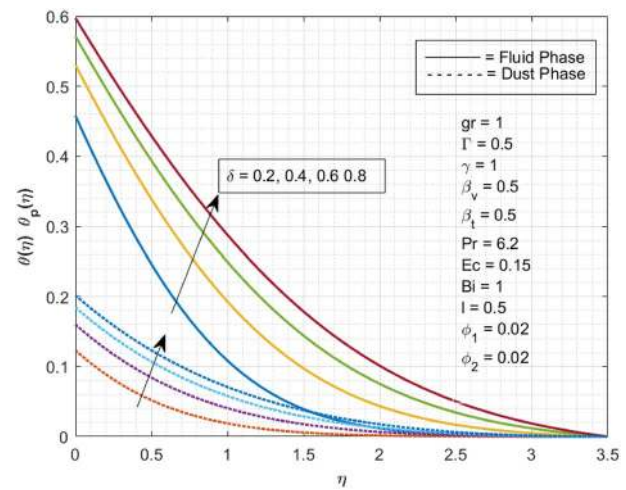


Fig. 6 Power of δ over $\theta(\eta), \theta_p(\eta)$

a display in Fig. 2. It is very clear from Fig. 2 that the liquid velocity is just as dust stage comparing to ($\delta = 0.2$) is least and the expansion of (δ) is to expand the velocity inside the boundary layer. Also ($\delta = 0$), the issue diminishes to flat surface. Henceforth, the speed inside the boundary layer on account of cylinder is bigger than the flat surface. It implies that the expanding in the cylinder measurement prompts the increasing in the velocity inside the boundary layer. The inclination in velocity gradient is faster in dust phase when compared to fluid phase. Figure 3 portrays the sway of gr on velocity gradient. The rise in values of gr gradually heightens the velocity of both the phases. Enhance in mixed convection parameter causes high difference in environmental and surface temperature. This difference causes increment in thermal gradient which

results in upshot of velocity in both the phases. The domination of mass concentration of the particle on thermal gradient of both phases is depicted in Fig. 4. One can detect from the figure that upsurge in l deteriorates the thermal profile. It is caused due to the dust particle mass concentration present in the liquid. Physically, it means that increasing value of l enhance the number density of dust particles and decelerate velocity of the dusty liquid and thermal gradient.

Figure 5 represents the encouragement of β_v on thermal gradient. It is detected from figure that upshot in β_v gradually boosts up the thermal profile. The dust phase boundary layer thickness is fewer than the thickness related with liquid phase as shown in Fig. 5. The sway of δ on thermal gradient is portrayed in Fig. 6. It is obvious from plotted figure that, upshot in curvature parameter progresses the thermal profile of both phases. Figure 7 shows the sway of Ec on thermal

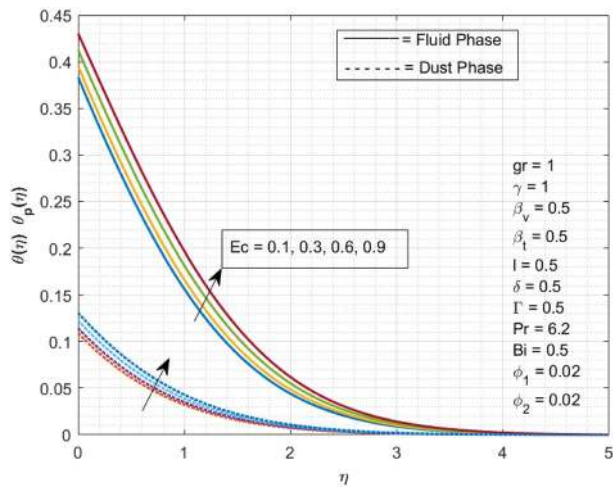


Fig. 7 Power of Ec over $\theta(\eta), \theta_p(\eta)$

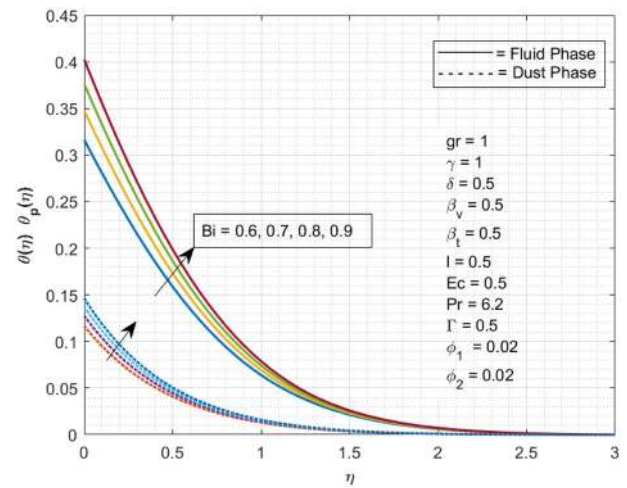


Fig. 9 Power of Bi over $\theta(\eta), \theta_p(\eta)$

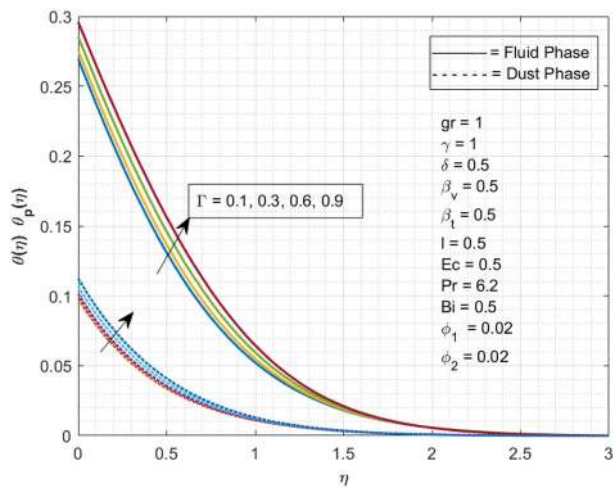


Fig. 8 Power of Γ over $\theta(\eta), \theta_p(\eta)$

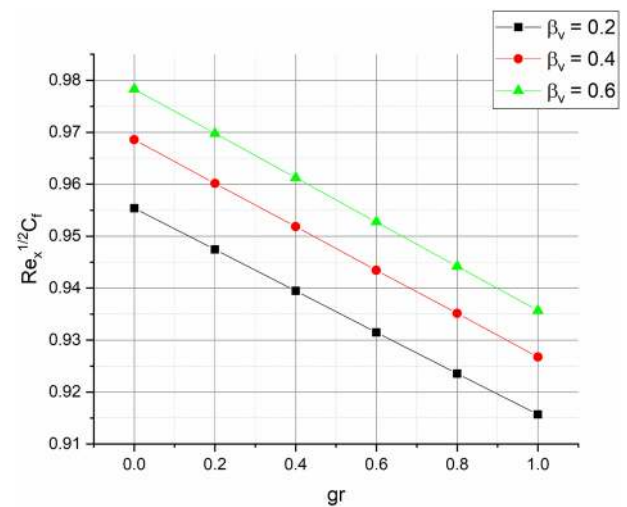


Fig. 10 Power of β_v on $Re_x^{1/2} C_f$

profile. It is observed from the plotted figure that heightening in Ec heightens the thermal gradient. It is obvious that, upsurge in Ec improve the inter-molecular motion and kinetic energy in fluid. As a result, this inter-molecular tension upsurgs the thermal gradient of both the phases and of the related boundary layer. The impact of Γ on thermal profile for both phases are displayed in Fig. 8. The heightening of Γ enhances the thermal profile of both phases as displayed in Fig. 8. The fluid phase boundary layer thickness is greater than the thickness related with dust phase. Physically, the existence of heat generation effects has the ability to enhance the thermal state of the liquid which reasons for an upsurge in its temperature and hence fluid phase is more thermal than dust phase. The sway of Bi on thermal profile for both the phases are displayed in Fig. 9. The measure of

the interaction among convection at its surface and conduction in the solid is called as Biot number. Here, it is essential to mention that, the extreme values of Bi enhances the thermal profile of both the phases. Here, the Bi comprises the heat transfer coefficient and which increases for higher values of Bi . Physically, inclination in Bi produces large heat transfer through convection which results in inclination of thermal field. Effect of β_v on $Re_x^{1/2} C_f$ is represented in Fig. 10. It is seen from figure that rise in values of β_v enhances the $Re_x^{1/2} C_f$. Figure 11 portrays the influence of l on $Re_x^{1/2} C_f$. One can observe from figure that rise in values of l enhances the $Re_x^{1/2} C_f$. Further, it is evident from both the figures that $Re_x^{1/2} C_f$ acts as a declining function of mixed convection parameter and growing function of l and β_v .

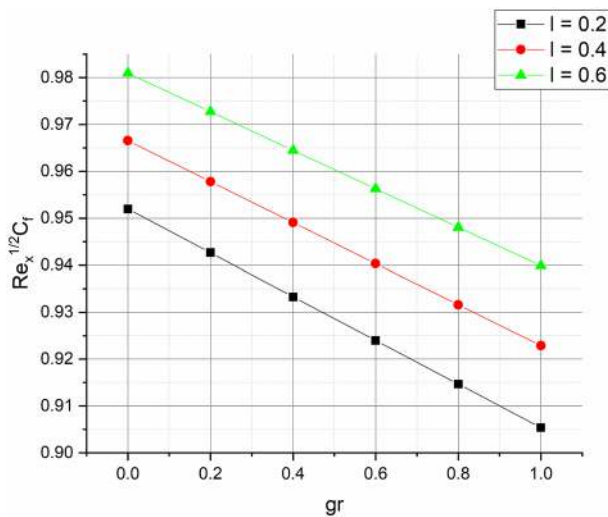


Fig. 11 Power of l on $Re_x^{1/2} C_f$

5 Final remarks

Numerically we discussed the dusty hybrid nanofluid flow through a stretching cylinder on taking account of mixed convection. The heat transference analysis is deliberated by using modified Fourier heat flux model. The suspension of Molybdenum disulphide and silver particles in base fluid water is considered in the current two-phase model. The framed equations arising in the current issue is minimized to ODE's by applying apt similarity variables. These reduced ODEs are numerically solved by using RKF-45 method by adopting shooting technique. The physical characteristics of velocity and thermal profiles of both fluid and dust phases have been deliberated under the influence of involved flow controlling physical parameters. The results conclude that, rise in values of mass concentration of particle declines the velocity and thermal gradient of dust and fluid phases. Upsurge in the diameter of cylinder leads to the increase in velocity and heat transfer within the boundary. The velocity of both the phases improves with increase in values of mixed convection parameter. Escalation in values of fluid–particle interaction parameter gradually enhances the thermal profile of both the phases. Further, improved values of mixed convection parameter declines the skin friction.

As stated in the introduction, various significant utilizations of this work are found in the polymer industry and thus later on we plan to broaden the investigation introduced here into non-Newtonian liquids in a different circumstance.

Funding The authors have no affiliation with any organization with a direct or indirect financial interest in the topic talked about in the manuscript.

Compliance with ethical standards

Conflict of interest The authors have no conflicts of interest to announce. All co-authors have seen and agree with the contents of the manuscript and there is no financial interest to report.

Open Access This article is licensed under a Creative Commons Attribution 4.0 International License, which permits use, sharing, adaptation, distribution and reproduction in any medium or format, as long as you give appropriate credit to the original author(s) and the source, provide a link to the Creative Commons licence, and indicate if changes were made. The images or other third party material in this article are included in the article's Creative Commons licence, unless indicated otherwise in a credit line to the material. If material is not included in the article's Creative Commons licence and your intended use is not permitted by statutory regulation or exceeds the permitted use, you will need to obtain permission directly from the copyright holder. To view a copy of this licence, visit <http://creativecommons.org/licenses/by/4.0/>.

References

- Hayat T, Qayyum S, Alsaedi A, Shafiq A (2016) Inclined magnetic field and heat source/sink aspects in flow of nanofluid with nonlinear thermal radiation. *Int J Heat Mass Transf* 103:99–107. <https://doi.org/10.1016/j.ijheatmasstransfer.2016.06.055>
- Khan JA, Mustafa M, Hayat T, Turkiymazoglu M, Alsaedi A (2017) Numerical study of nanofluid flow and heat transfer over a rotating disk using Buongiorno's model. *Int J Numer Methods Heat Fluid Flow* 27(1):221–234. <https://doi.org/10.1108/HFF-08-2015-0328>
- Kuttan BA, Manjunatha S, Jayanthi S, Giresha BJ (2020) Performance of four different nanoparticles in boundary layer flow over a stretching sheet in porous medium driven by buoyancy force. *Int J Appl Mech Eng* 25(2):1–10. <https://doi.org/10.2478/ijame-2020-0016>
- Vinita V, Poply V (2020) Impact of outer velocity MHD slip flow and heat transfer of nanofluid past a stretching cylinder. *Mater Today Proc* 26:3429–3435. <https://doi.org/10.1016/j.matpr.2019.11.304>
- Mondal H, Das S, Kundu PK (2020) Influence of an inclined stretching cylinder over MHD mixed convective nanofluid flow due to chemical reaction and viscous dissipation. *Heat Transf* 49(4):2183–2193. <https://doi.org/10.1002/hjt.21714>
- Khan MI, Ahmad Khan S, Hayat T, Waqas M, Alsaedi A (2019) Modeling and numerical simulation for flow of hybrid nanofluid (SiO₂/C₃H₈O₂) and (MoS₂/C₃H₈O₂) with entropy optimization and variable viscosity. *Int J Numer Methods Heat Fluid Flow* 30(8):3939–3955. <https://doi.org/10.1108/HFF-10-2019-0756>
- Farooq S, Ijaz Khan M, Waqas M, Hayat T, Alsaedi A (2020) Transport of hybrid type nanomaterials in peristaltic activity of viscous fluid considering nonlinear radiation, entropy optimization and slip effects. *Comput Methods Progr Biomed* 184:105086. <https://doi.org/10.1016/j.cmpb.2019.105086>
- Manjunatha S, Ammani Kuttan B, Ramesh GK, Giresha BJ, Aly EH (2020) 3D flow and heat transfer of micropolar fluid suspended with mixture of nanoparticles (Ag-CuO/H₂O) driven by an

- exponentially stretching surface. *Multidiscip Model Mater Struct* 16(6):1691–1707. <https://doi.org/10.1108/MMMS-12-2019-0226>
9. Abbas N, Nadeem S, Saleem A, Malik MY, Issakhov A, Alharbi FM (2021) Models base study of inclined MHD of hybrid nanofluid flow over nonlinear stretching cylinder. *Chin J Phys* 69:109–117. <https://doi.org/10.1016/j.cjph.2020.11.019>
 10. Turkiilmazoglu M (2017) Magnetohydrodynamic two-phase dusty fluid flow and heat model over deforming isothermal surfaces. *Phys Fluids* 29(1):013302. <https://doi.org/10.1063/1.4965926>
 11. Manjunatha PT, Giresha BJ, Prasannakumara BC (2017) Effect of radiation on flow and heat transfer of MHD dusty fluid over a stretching cylinder embedded in a porous medium in presence of heat source. *Int J Appl Comput Math* 3(1):293–310. <https://doi.org/10.1007/s40819-015-0107-x>
 12. Gnaneswara Reddy M, Sudha Rani MVNL, Ganesh Kumar K, Prasannakumar BC, Lokesh HJ (2020) Hybrid dusty fluid flow through a Cattaneo-Christov heat flux model. *Phys Stat Mech Appl* 551:123975. <https://doi.org/10.1016/j.physa.2019.123975>
 13. Radhika M, Gowda RJP, Naveenkumar R, Siddabasappa BCP (2020) Heat transfer in dusty fluid with suspended hybrid nanoparticles over a melting surface. *Heat Transf.* <https://doi.org/10.1002/htj.21972>
 14. Mallikarjuna HB, Nirmala T, Gowda RJP, Manghat R, Kumar RSV (2021) Two-dimensional Darcy-Forchheimer flow of a dusty hybrid nanofluid over a stretching sheet with viscous dissipation. *Heat Transf.* <https://doi.org/10.1002/htj.22058>
 15. Abdelmalek Z, Nawaz M, Elmasry Y (2020) Simultaneous impact of hybrid nano and dust particles on enhancement of heat transfer in fluid with micro-rotation and thermal memory effects. *Int Commun Heat Mass Transf* 118:104871. <https://doi.org/10.1016/j.icheatmasstransfer.2020.104871>
 16. Hayat T, Qayyum S, Alsaedi A, Asghar S (2017) Radiation effects on the mixed convection flow induced by an inclined stretching cylinder with non-uniform heat source/sink. *PLoS ONE* 12(4):e0175584. <https://doi.org/10.1371/journal.pone.0175584>
 17. Khan MI, Tamoor M, Hayat T, Alsaedi A (2017) MHD boundary layer thermal slip flow by nonlinearly stretching cylinder with suction/blowing and radiation. *Results Phys* 7:1207–1211. <https://doi.org/10.1016/j.rinp.2017.03.009>
 18. Waqas M, Naz S, Hayat T, Alsaedi A (2019) Numerical simulation for activation energy impact in Darcy-Forchheimer nanofluid flow by impermeable cylinder with thermal radiation. *Appl Nanosci* 9(5):1173–1182. <https://doi.org/10.1007/s13204-018-00940-z>
 19. Mishra A, Kumar M (2020) Velocity and thermal slip effects on MHD nanofluid flow past a stretching cylinder with viscous dissipation and Joule heating. *SN Appl Sci* 2(8):1350. <https://doi.org/10.1007/s42452-020-3156-7>
 20. Qayyum S, Hayat T, Shehzad SA, Alsaedi A (2018) Mixed convection and heat generation/absorption aspects in MHD flow of tangent-hyperbolic nanofluid with Newtonian heat/mass transfer. *Radiat Phys Chem* 144:396–404. <https://doi.org/10.1016/j.radphyschem.2017.10.002>
 21. Alsaedi A, Hayat T, Qayyum S, Yaqoob R (2020) Eyring–Powell nanofluid flow with nonlinear mixed convection: Entropy generation minimization. *Comput Methods Progr Biomed* 186:105183. <https://doi.org/10.1016/j.cmpb.2019.105183>
 22. Akbar Y, Abbasi FM, Shehzad SA (2020) Thermodynamical analysis for mixed convective peristaltic motion of silver-water nanofluid having temperature dependent electrical conductivity. *Appl Nanosci.* <https://doi.org/10.1007/s13204-020-01569-7>
 23. Ramesh GK, Manjunatha S, Roopa GS, Chamkha AJ (2020) Hybrid (ND-Co3O4/EG) nanofluid through a permeable cylinder under homogeneous-heterogeneous reactions and slip effects. *J Therm Anal Calorim.* <https://doi.org/10.1007/s10973-020-10106-1>
 24. Salahuddin T, Malik MY, Hussain A, Bilal S, Awais M (2016) MHD flow of Cattaneo–Christov heat flux model for Williamson fluid over a stretching sheet with variable thickness: using numerical approach. *J Magn Magn Mater* 401:991–997. <https://doi.org/10.1016/j.jmmm.2015.11.022>
 25. Ijaz Khan M, Nigar M, Hayat T, Alsaedi A (2020) On the numerical simulation of stagnation point flow of non-Newtonian fluid (Carreau fluid) with Cattaneo–Christov heat flux. *Comput Methods Progr Biomed* 187:105221. <https://doi.org/10.1016/j.cmpb.2019.105221>
 26. Hussain A, Malik MY, Khan M, Salahuddin T (2019) Application of generalized Fourier heat conduction law on MHD viscoelastic fluid flow over stretching surface. *Int J Numer Methods Heat Fluid Flow* 30(6):3481–3496. <https://doi.org/10.1108/HFF-02-2019-0161>
 27. Ahmed A, Khan M, Ahmed J, Nadeem S (2020) Mixed convection in unsteady stagnation point flow of maxwell fluid subject to modified Fourier’s Law. *Arab J Sci Eng* 45(11):9439–9447. <https://doi.org/10.1007/s13369-020-04724-y>
 28. Khan M, Ahmed A, Irfan M, Ahmed J (2020) Analysis of Cattaneo-Christov theory for unsteady flow of Maxwell fluid over stretching cylinder. *J Therm Anal Calorim.* <https://doi.org/10.1007/s10973-020-09343-1>
 29. Grubka LJ, Bobba KM (1985) Heat transfer characteristics of a continuous stretching surface with variable temperature. *ASME J Heat Transf* 107(1):248–250
 30. Abel MS, Mahesha N (2008) Heat transfer in MHD viscoelastic fluid flow over a stretching sheet with variable thermal conductivity, non-uniform heat source and radiation. *Appl Math Model* 32(10):1965–1983
 31. Ali ME (1994) Heat transfer characteristics of a continuous stretching surface. *Wärme- Stoffübertrag* 29(4):227–234
 32. Ishak A, Nazar R, Pop I (2008) Hydromagnetic flow and heat transfer adjacent to a stretching vertical sheet. *Heat Mass Transf* 44(8):921
 33. Shafie S, Gul A, Khan I (2016) Molybdenum disulfide nanoparticles suspended in water based nanofluids with mixed convection and flow inside a channel filled with saturated porous medium. *AIP Conf Proc* 1775(1):030042
- Publisher’s Note** Springer Nature remains neutral with regard to jurisdictional claims in published maps and institutional affiliations.